J Appl Electrochem (2010) 40:791–797
DOI 10.1007/s10800-009-0058-1

Determination of hydrogenation ability and exchange current of H_2O/H_2 system on hydrogen-absorbing metal alloys

Henryk Bala · Krystyna Giza · Iwona Kukula

Received: 20 May 2009 / Accepted: 8 December 2009 / Published online: 13 December 2009

Abstract A detailed analysis of potential versus time measurements at galvanostatic charge/discharge conditions (external current change from -1 to $+1$ mA cm^{-2}) for two La–Ni alloys in Ar-saturated 0.1 M KOH solution is presented. It is shown that passivation of the electrodes does not affect the potential jump as a result of current switching over. The value of potential jump allows to calculate the exchange current density for H_2O/H_2 system on the tested material. Anodic potential of the hydrogenated electrode (at $i_a = \text{const}$) linearly increases with logarithm of time which allows to evaluate precisely time necessary for oxidation of hydrogen absorbed during cathodic charging. The method described enables to determine effectiveness of hydrogen absorption by materials applied for negative electrodes of NiMH batteries.

Keywords Hydrogen storage alloys · $-i/+i$ Galvanostatic curves · Exchange current density · Absorption/desorption of hydrogen · Hydrogen absorption efficiency

1 Introduction

In recent years, many different R–T type intermetallic alloys and compounds (R = rare earth element, T = transition metal) are considered as possible negative electrode materials for metal-hydride batteries [1–3]. Among these compounds RT_5, RT_3 and R_2T_7 seem to be most prospective. In order to increase hydrogen capacity and rate of charge/discharge process above mentioned alloys are being modified usually by partial substitution of both R (by another rare-earth metal) and T (by other d-electron metal) [4–6]. It is worth noting that interesting properties can also be obtained by partial substitution of T by metallic- or non-metallic elements of main groups (III–V) of periodic table of elements [4–9].

There are plenty of different experimental methods for testing of hydrogenation ability of materials. These methods include hydrogenation from gaseous phase (p–c isotherms) [10–12], hydrogen high-temperature desorption [13], electrochemical measurements (charge–discharge curves [14–16], hydrogen permeation through metal membranes [17, 18], polarisation curves [19–21], polarisation resistance [22]), mass spectrometry [23] or thermomagnetic measurements [24]. One of the most simple and promising is galvanostatic charge–discharge method which allows to evaluate and compare electrical charge necessary for oxidation of cathodically evolved and absorbed hydrogen. Time necessary for hydrogen oxidation at constant anodic current density can be a relevant measure of amount of hydrogen absorbed earlier during cathodic charging [22, 25–28]. It turns, however, that there is a possibility to obtain much more valuable information relating effectiveness and kinetics of hydrogenation process on the basis of galvanostatic charge/discharge curves as compared to these published so far.

In this article, a thorough analysis of galvanostatic charge/discharge curves is described and possibilities for drawing further information from their plots are discussed. Because the method consists in rapid change of sign of external current after sample hydrogenation, in further parts of this article, it is called "$-i/+i$ method".

H. Bala · K. Giza (✉) · I. Kukula
Department of Chemistry, Czestochowa University of Technology, Al. Armii Krajowej 19, 42-200 Czestochowa, Poland
e-mail: giza@mim.pcz.czest.pl

2 Theoretical analysis of constant current pulse for hydrogen electrode

2.1 Reversible H_2O/H_2 reaction on inert electrode

A number of metals and alloys absorb hydrogen both from gaseous phase (H_2) or cathodically evolved, which enters the metal crystal lattice in atomic form. The absorption process consists of some stages. First of them is physisorption of H_2 molecules and then chemisorption of hydrogen atoms on the metal surface [29, 30]. Adsorbed H_{ads} atoms may enter the metal lattice to produce hydrogen solid solution or metal hydride. These two forms of hydrogen inside the metal crystal lattice can be called generally "absorbed hydrogen". In real metallic materials a considerable part of absorbed hydrogen involves also so called *trapped hydrogen*, connected with structural gaps. In case the hydrogenated metal alloy is in contact with aqueous solution, the process of alloy hydrogenation/dehydrogenation becomes a *redox* process, and the rate of both partial processes depends on electrode potential. In order to avoid corrosion of electrode material, in particular for NiMH batteries, aqueous solutions of concentrated alkaline solutions are applied. In such solutions, most of metallic materials reveal acceptable stability owing to effective passivation [31–33].

As a slow electrochemical step for most of the metals, the one-electron transfer is generally accepted for alkaline media:

$$\text{Anodic process: } H_{ads} + OH^- - e \xrightarrow{i_a} H_2O \tag{1a}$$

$$\text{Cathodic process: } H_2O + e \xrightarrow{i_c} H_{ads} + OH^- \tag{1b}$$

Adsorbed hydrogen atoms may then combine to produce H_2 molecules or enter the crystal lattice (absorption). Hydrogen molecules dissolve in aqueous solution and, after reaching saturation, they form hydrogen bubbles and leave the metal surface. This equilibrium can be written as follows:

$$2H_{abs} \rightleftarrows 2H_{ads} \rightleftarrows H_{2(\text{dissolved})} \rightleftarrows H_{2(g)} \tag{2}$$

In conditions of saturation of solution with hydrogen-gas, its pressure over the solution is equal to the external pressure. For hydrogen bubbles generated on the metal surface in atmospheric conditions, one can assume that $p_{H_2} = 1\,\text{atm}$, and the equilibrium potential for H_2O/H_2 system is

$$E^{eq}_{H_2O/H_2} = -0.059\text{pH} - 0.059 \log p^{1/2}_{H_2} \tag{3}$$

At constant p_{H_2}(and equal to 1 atm), the equilibrium potential of hydrogen electrode decreases from 0.00 V (for pH = 0) to −0.827 V (for pH = 14). Similarly, at constant pH, the $E^{eq}_{H_2O/H_2}$ increases with a decrease of p_{H_2}. In equilibrium state, the anodic (i_a) and cathodic (i_c) processes occur with the same rate, equal to the exchange current density:

$$i_a = |i_c| = i^o_{H_2O/H_2} \tag{4}$$

For solid, thick metal electrodes, the rates of electrochemical processes are expressed in current density units, most commonly in A cm^{-2}. For thin films of electrode materials or for powdered electrodes it is also advantageous to express the current density in A g^{-1}. The exchange current density depends on kind of the electrode material and, generally, characterizes the kinetics of electrochemical hydrogen reaction [19, 27, 30, 34]. The greater $i^o_{H_2O/H_2}$ value, the larger amounts of hydrogen can be oxidized in chosen period of time. Consequently, the greater $i^o_{H_2O/H_2}$ values, the larger currents can be derived from the MH battery without substantial change in its voltage.

Rates of partial electrode processes (1a) and (1b), according to fundamentals of electrochemical kinetics [34, 35], are

$$i_a = k_a p^{1/2}_{H_2} \exp\frac{\alpha FE}{RT} \tag{5a}$$

$$i_c = -k_c[H^+] \exp\left(-\frac{(1-\alpha)FE}{RT}\right) \tag{5b}$$

where k_a and k_c are rate constants, α is a symmetry factor, usually equal to 0.5, R is the gas constant, F is the Faraday constant, T is the absolute temperature, and E is the electrode potential. For $E = E^{eq}_{H_2O/H_2}$, Eq 4 obeys. When we denote $E - E^{eq}_{H_2O/H_2} = \eta$ ($\eta \equiv$ overpotential) and $\alpha = 0.5$, the Eqs. 5a, 5b take on more simple forms:

$$i_a = i^o \exp B\eta \tag{6a}$$

and

$$i_c = -i^o \exp(-B\eta) \tag{6b}$$

where $B = \frac{F}{2RT}$. After some transformations, we obtain Tafel equations:

$$E = A \pm b \log i \tag{7a}$$

or

$$\eta = A' \pm b \log i \tag{7b}$$

where b is a Tafel slope of the H_2O/H_2 system, equal to 0.12 V for most of the electrode materials.

In Fig. 1, simplified plots of partial polarisation curves, i.e. $E = f(\log i)$ dependencies, for anodic (a and a') and cathodic (c and c') polarisation curves of hydrogen electrode (H_2O/H_2 system) in case of low (a' and c') and high (a and c) exchange current densities are presented. The polarisation dependencies presented in Fig. 1 (so called *Evans diagrams*)

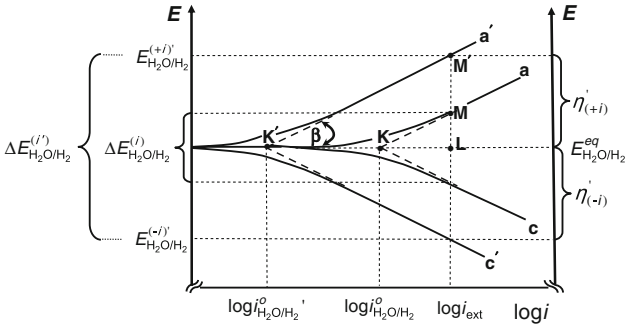

Fig. 1 Evans diagram for hydrogen electrode on two different metals. Details relating symbols in text

have been plotted analogously as in classic electrochemical works, e.g. in [34, 35]. The solid lines in Fig. 1 are the sums of partial anodic and cathodic straight lines in semilogarithmic coordinate system. In the figure, two situations are considered for hydrogen electrode at the same pH and p_{H_2}, but the electrode process occurs on two different metallic materials. Thus equilibrium potential of H_2O/H_2 system is the same on both surfaces, but there are differences in exchange current densities $\left(i^{o}_{H_2O/H_2}{}' < i^{o}_{H_2O/H_2}\right)$. It is also assumed that mechanisms of partial electrode processes are the same on both surfaces, so the partial polarisation curves are parallel ($b_a = b'_a$ and $b_c = b'_c$).

Let us assume that the hydrogen electrode is cathodically polarised by passing an external current, equal to i_{ext}, through it [the cathodic current $(-i)$ has its negative value, but because of logarithm finding requirements, the i_{ext} is its absolute value]. The electrode potential will be moved towards negative direction by $\eta_{(-i)}$ and will take on a value of $E^{(-i)}_{H_2O/H_2}$. Analogously, in case of anodic polarisation of the electrode and passing a positive current through it ($i_{ext} = +i$), we bring about electrode potential increase by $\eta_{(+i)}$ and its settling down at $E^{(+i)}_{H_2O/H_2}$. As it is seen from Fig. 1, the difference of $E^{(+i)}_{H_2O/H_2} - E^{(-i)}_{H_2O/H_2} = \Delta E^{(i)}_{H_2O/H_2}$ is the greater, the smaller exchange current density of the H_2O/H_2 system.

In order to find a correlation between $\Delta E^{(i)}$ and logi^o let we consider a triangle KLM or K′LM′ in Fig. 1. Because the partial electrode processes are symmetric to each other ($\alpha = 0.5$), we can assume the Tafel slopes to be $b_a = b_c = \mathrm{tg}\beta$.

$$\mathrm{tg}\beta = \frac{\mathrm{LM}}{\mathrm{KL}} = \frac{\frac{1}{2}\Delta E^{(i)}}{\log i_{ext} - \log i^{o}} \tag{8}$$

from which

$$\log i^{o} = \log i_{ext} - \frac{\Delta E^{(i)}}{2b_a} \tag{8a}$$

or, assuming $i_{ext} = 1$ mA cm^{-2} and $b_a = b_c = 0.12$ V, we get

$$\log i^{o}_{H_2O/H_2} = -\frac{\Delta E^{(1)}_{H_2O/H_2}}{0.24} \tag{8b}$$

where $\Delta E^{(1)}_{H_2O/H_2}$ is expressed in (V) and $i^{o}_{H_2O/H_2}$ in (mA cm^{-2}).

The Eq. 8b holds well for simple H_2O/H_2 electrode, i.e. in case of absence any other electrode processes on the metal surface. Indirectly, one can confirm that the system considered behaves nearly as a simple hydrogen electrode when

$$E^{eq}_{H_2O/H_2} = \frac{E^{(+i)}_{H_2O/H_2} + E^{(-i)}_{H_2O/H_2}}{2} \tag{9}$$

However, there appear sometimes experimental difficulties to measure the equilibrium potential with sufficient accuracy, resulting from existence of diffusion potentials in reference electrode, specific differences in p_{H_2} values at cathodic- and anodic polarisation, certain near-surface pH changes, especially in diluted solutions, etc.

The relationships (8)–(8b) are still valid also for hydrogen electrodes that undergo any other "background" reactions, which are, however, not very fast. First of all, we should consider the effect of passivation of electrode material, which is very common for R–T negative electrodes in NiMH-type batteries. Anodic passivation currents ($i_{a,pas}$) in these systems in strong alkaline solutions are on the level of 0.1–0.3 mA cm^{-2} [33, 36]. In Fig. 2, two Evans diagrams are presented at assumption that $i_{a,pas} = \frac{1}{20} i_{ext}$ (A) or $i_{a,pas} = \frac{1}{5} i_{ext}$ (B). The electrode OCP potential (resultant potential $E^{res}_{H_2O/H_2}$) corresponds to the situation when $i_{a,H_2O/H_2} + i_{a,pas} = i_{c,H_2O/H_2}$, and

$$E^{res(pas)}_{H_2O/H_2} < E^{eq}_{H_2O/H_2} \tag{10}$$

The thorough analysis of polarisation curves presented in Fig. 2 shows, however, that the difference of potentials caused by passing of $(-i)$ and $(+i)$ currents remains practically unchangeable unless the passive anodic currents are too big:

$$\Delta E^{(i)}_{H_2O/H_2} \cong \Delta E^{(i),pas}_{H_2O/H_2} \tag{10a}$$

The calculations show that Eq. 10a holds good when $i_{a,pas} \le i_{ext}$. Taking into consideration that for real R–T electrodes in alkaline solutions, $i_{a,pas}$ are on the order of 0.1 mA cm^{-2}, one can expect that the discussed potential difference will be constant in case of applying external currents of ± 1.0 mA cm^{-2}.

Similarly as in case of electrode passivation, in the presence of limiting current of O_2 reduction Eq. 8b holds well when $i_{O_2,lim} \le i_{ext}$, and it is easy to prove that $E^{res(O_2)}_{H_2O/H_2} > E^{eq}_{H_2O/H_2}$ in such a case. Of course, for argon-saturated solutions, $i_{O_2,lim}$ is negligible, even at very rapid stirring rates.

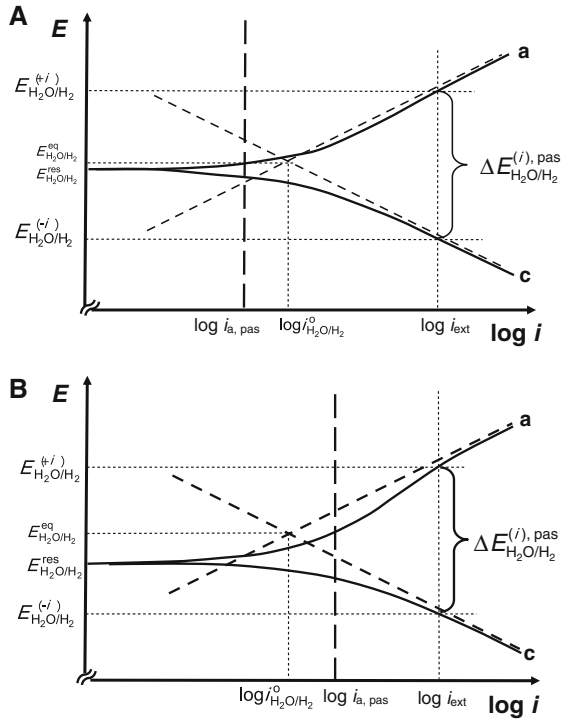

Fig. 2 Evans diagrams for H_2O/H_2 system on the surface of passivating material. It is assumed that external $\pm i_{ext}$ current density is 10 times less than the exchange current density for the hydrogen electrode. Anodic passivation current $i_{a,pas}$ is equal to $\frac{1}{20}i_{ext}$(A) or $\frac{1}{5}i_{ext}$(B)

2.2 Galvanostatic $-i/+i$ relationships for H_2O/H_2 system

Anodic Tafel behaviour (curves *a* and *a′* in Fig. 1) occurs for hydrogen electrode in case of presence of hydrogen gas at the electrode surface. The source of hydrogen gas can be either external H_2-scrubber or the hydrogenated electrode (solid solution of atomic hydrogen in crystal lattice). In case, the test solution is saturated with inert gas (e.g. argon), the process of anodic oxidation of hydrogen absorbed by the electrode material in cathodic cycle occurs until all hydrogen atoms leave the electrode crystal lattice, and, consequently, $p_{H_2} = 0$. As it can be concluded from Eq. 3, equilibrium potential of hydrogen electrode moves towards positive values with p_{H_2} decrease. Equilibrium concentration of atomic hydrogen in the metal crystal lattice (c_H) depends on p_{H_2} according to Sievert's relation [37, 38]

$$c_H = k p_{H_2}^{\frac{1}{2}} \exp\left(-\frac{\Delta H_{sol}}{RT}\right) \tag{11}$$

where ΔH_{sol} is the enthalpy of hydrogen dissolution in the material and k is the constant dependent on lattice structure. For very thick electrodes (>1 mm), the time necessary to attain the equilibrium may be comparatively long, however, Eq. 11 holds well for hydrogenated subsurface layers of the electrode material.

From Eq. 5a, one can get the following equation for electrode potential at external anodic current equal to i_{ext}:

$$E_{H_2O/H_2}^{(+i)} = \frac{2.3RT}{\alpha F}\left(-\log k_a - \log p_{H_2}^{\frac{1}{2}} + \log i_{ext}\right) \tag{12}$$

Such a value of electrode potential applies well directly after switching the external current from negative to positive value (i.e. from $-i_{ext}$ to $+i_{ext}$).

For galvanostatic conditions, i_{ext} and k_a values are constant, however, $p_{H_2}^{\frac{1}{2}}$ decreases with time (because hydrogen oxidizes anodically), so the Eq. 12 can be written in the following form:

$$E_{H_2O/H_2}^{(+i)}(t) = A - b_a \log p_{H_2}^{\frac{1}{2}} \tag{12a}$$

where $b_a = 2.3RT/(\alpha F)$ and $A = b_a \log \frac{i_{ext}}{k_a}$. Directly after $-i/+i$ switching, p_{H_2} on the surface is 1 atm, thus $E_{H_2O/H_2}^{(+i)} = A$. Anodic oxidation of hydrogen absorbed is prone to the decrease of c_H in electrode subsurface layer and, hence, to the decrease of p_{H_2} at the metal/solution interface (according to Eq. 11), and, consequently, to the movement of $E_{H_2O/H_2}^{(+i)}$ potential towards positive values. In practice, for $i_{ext} = 1$ mA cm^{-2}, the increase of $E_{H_2O/H_2}^{(+i)}$ potential begins after a fraction of second up to a few seconds.

The depth profile of hydrogen concentration lay-out in the electrode material depends on charging conditions, and it certainly strongly changes when the external current is switched over. The mathematical form of the change of hydrogen concentration in subsurface layers (c_H) versus time is not known; however, analysis of large number of experiments made by authors of the paper allows to assume that within a few seconds after the $-i/+i$, switching the following empirical relationship holds good:

$$c_H = \frac{k'}{t^n} \tag{13}$$

where k' and n are constants which should be determined experimentally. The greater the power coefficient n, the stronger is the drop of hydrogen concentration with time. Analogous hyperbolic dependence has been found for hydrogen oxidation rate versus time in potentiostatic conditions [28, 39, 40]. From dependencies (11)–(13), we finally get

$$E_{H_2O/H_2}^{(+i)}(t) = B + n b_a \log t \tag{14}$$

where B is a new constant that includes k, k_a, ΔH_{sol}, b_a and i_{ext} constants and $B \geq A$. As it results from Eq. 14, the constant B is equal to $E_{H_2O/H_2}^{(+i)}$ ($t = 1$ s)

In Fig. 3, the theoretical plot for the galvanostatic $-i/+i$ measurement on inert, non-passivating metal surface is presented. It is assumed that directly after cathodic

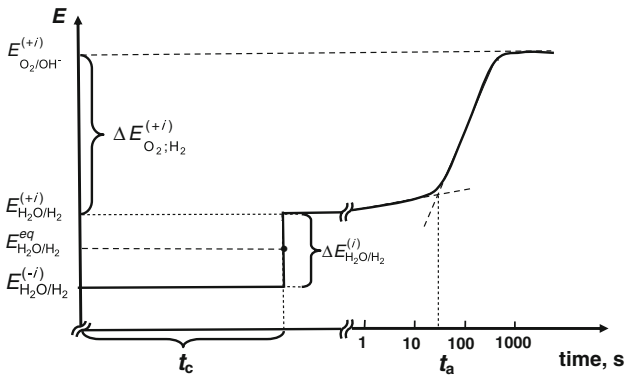

Fig. 3 Theoretical galvanostatic $-i/+i$ plot for H_2O/H_2 system on non-passivating electrode capable to absorb hydrogen. Details relating symbols see text

hydrogenation (i.e. after time t_c), the sign of external current is rapidly changed and electrode potential jumps from $E^{(-i)}$ to $E^{(+i)}$. After a few seconds, potential starts to increase linearly with log t, according to Eq. 14, and the time for oxidation of hydrogen (absorbed in cathodic cycle) is t_a. After time necessary for oxidizing all hydrogen absorbed by metal, the further, sharp increase of electrode potential is visible up to anodic evolution of oxygen ($E^{(+i)}_{O_2/OH^-}$). It is shown in Fig. 3 how to determine graphically the most important parameters characterizing hydrogen absorption ability: $\Delta E^{(i)}_{H_2O/H_2}$ and t_a.

3 Results and discussion

In Fig. 4, experimental $-i/+i$ galvanostatic curves for two La–Ni alloys ($LaNi_5$ and La_3Ni) are presented. $LaNi_5$ is a well-known intermetallic compound that is able to absorb large amounts of hydrogen (*ca* 6 mol H per formula unit [6, 10–12]), whereas La_3Ni eutectic alloy possesses no ability to absorb hydrogen effectively [33]. The experiments were

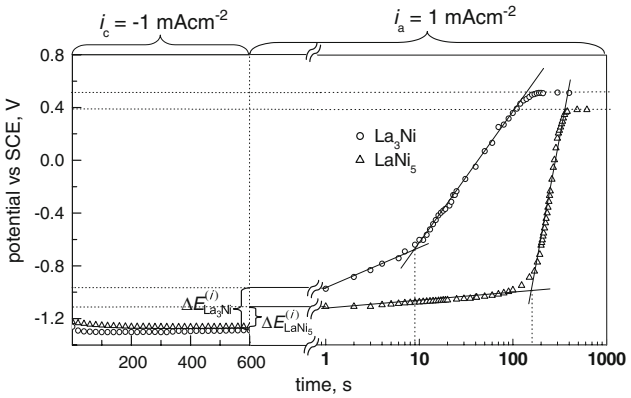

Fig. 4 Galvanostatic charge/discharge curves ($-i/+i$ dependencies) for two La-Ni alloys in deaerated, 0.1 M KOH solution ($i_c = -1.0$ mA cm^{-2}, $i_a = +1.0$ mA cm^{-2}, 25 °C, Ar, 15 rps)

carried out in diluted, 0.1 M KOH solution to avoid nickel and lanthanum hydroxides dissolution (to produce $HNiO_2^-$ or La^{3+} ions, respectively) or nickel transpassivation (to produce $Ni(OH)_4^-$) [31]. Solutions were thermostated (25 °C) and saturated with high purity argon (99.99%) with a rate of 2 L min^{-1}. Electrodes of $LaNi_5$ and La_3Ni alloys had a shape of rotating discs with an operating surface area of 0.1 cm^2. In polarisation experiments fast stirring rate (15 rev s^{-1}) was applied to avoid surface screening by gas bubbles (H_2 at cathodic and O_2 at highly anodic potentials). After polishing (waterproof emery paper No 1000), rinsing in water and in alcohol the eventually dried working electrode was hydrogenated galvanostatically with cathodic current $i_c = -1.0$ mA cm^{-2}, during $t_c = 600$ s. Then, the electrode polarization was being rapidly changed into $i_a = +1.0$ mA cm^{-2} ($-i/+i$ overswitching). During the experiment, the electrode potential was continuously registered. The cathodic potential $E^{(-i)}_{H_2O/H_2}$ used to reach its steady state value usually after 100–200 s. When the external current was switched over into +1.0 mA cm^{-2}, the significant, sudden potential jump ($\Delta E^{(i)}_{H_2O/H_2}$) into anodic direction was observed every time, and the anodic potential was constant within approx. 1 s. Then, potential started to increase linearly with log t, according to Eq. 14. After electrode full dehydrogenation, i.e. after time t_a (see Figs. 3 and 4), the second sharp potential jump was registered ($\Delta E^{(+i)}_{O_2;H_2}$), until the electrode achieved potential of oxygen evolution ($E^{(+i)}_{O_2/OH^-}$). Both potential jumps exhibit their linear character versus log t, which facilitates precise determination of t_a periods for both kinds of La–Ni samples. In Table 1, the values of parameters resulting from Fig. 4 for both electrode materials are presented. Hydrogenation absorption coefficient (γ_{eff}) determines the part of hydrogen evolved that enters the sample crystal lattice [28, 39], and it is defined as

$$\gamma_{eff} = \frac{q_{H,ox}}{q_{H^+,red}} \tag{15}$$

where $q_{H,ox}$ and $q_{H^+,red}$ are charges for oxidation of absorbed hydrogen atoms and for reduction of H^+ (or H_2O) molecules, respectively. In case the external cathodic and anodic currents have the same absolute values, the γ_{eff} equals to t_a/t_c.

In practice, hydrogenation effectiveness is usually greater than that determined from the Eq. 15 because the anodic charge does not bear in mind the trapped hydrogen. One may also expect that hydrogenation effectiveness will be greater for not agitated solutions. As it has been mentioned earlier, rapid stirring allows to avoid the surface screening by gas bubbles, which improves the accuracy of the measurements. On the other hand, however, fast detachment of H_2 bubbles from the surface may also limit in certain degree hydrogenation of the material.

Table 1 Numerical values of parameters describing efficiency of cathodic hydrogenation resulting from Eqs. 8, 10 and 14. Hydrogenation absorption coefficient (γ_{eff}) determines part of hydrogen evolved that enters the sample crystal lattice

Sample	$\Delta E^{(i)}_{H_2O/H_2}$ (V)	$i^o_{H_2O/H_2}$ (mA cm^{-2})	t_a (s)	$\gamma_{eff} = \left(\frac{t_a}{t_c}\right) \cdot 100\%$ (%)	$\left(\frac{\partial E^{(+i)}_{H_2O/H_2}}{\partial \log t}\right)_{+i}$ (V)	n
$LaNi_5$	0.323	0.045	157	26.2	0.072	0.61
La_3Ni	0.477	0.010	9.0	1.5	0.33	2.80

As it was shown in our earlier papers [20, 28, 33, 36], both $LaNi_5$ and La_3Ni alloys easily passivate in KOH solutions and anodic currents in passive range were in the range of 0.3–0.6 mA cm^{-2} (for $LaNi_5$) and 0.01–0.03 mA cm^{-2} (for La_3Ni), i.e. the $i_{a,pas}$ currents are clearly smaller than the absolute values of applied external currents ($i_c = -1.0$ and $i_a = +1.0$ mA cm^{-2}). Owing to passing argon by the solution, the limiting current of oxygen reduction was practically negligible ($\ll 10^{-2}$ mA cm^{-2}) in spite of electrode very fast rotation speed.

Due to passivation, the average electrode potential determined from potential values at $+i$ and $-i$ currents cannot be a measure of equilibrium potential (Eq. 9) but rather resultant potential $E^{res(pas)}_{H_2O/H_2}$ (see Eq. 10). It can be read from Fig. 4 that $E^{res(pas)}_{H_2O/H_2}$ values (vs. SCE) are -1.20 and -1.11 V for $LaNi_5$ and La_3Ni alloys, respectively. The theoretical value of equilibrium potential for H_2O/H_2 system at pH = 13 and $p_{H_2} = 1$atm is -1.01 V (vs. SCE), i.e. the $E^{res(pas)}_{H_2O/H_2}$ potentials are evidently more negative than $E^{eq}_{H_2O/H_2}$, which is consistent with theoretical predictions for passivating electrode (compare Eq. 10).

Comparison of data presented in Table 1 allows to conclude that hydrogen absorption efficiency is much greater for $LaNi_5$ alloy (26.2%) than that for La_3Ni (1.5% only). According to expectations, exchange current density of H_2O/H_2 electrode is distinctly greater on $LaNi_5$ surface than that for La_3Ni.

As it is known, difference between equilibrium potentials of H_2O/H_2 and O_2/OH^- electrodes should be 1.23 V (at pH = const and at $p = 1$ atm). It is easy to prove that in case of $b_{a,H_2O/H_2} = b_{a,O_2/OH^-} = 0.12$ V and at the same i^o values of both of the redox systems, the difference between $E^{(+i)}_{O_2/OH^-}$ and $E^{(+i)}_{H_2O/H_2}$ values should also be equal to 1.23 V. As it can be read from Fig. 4, the $E^{(+i)}_{O_2/OH^-} - E^{(+i)}_{H_2O/H_2} = \Delta E^{(+i)}_{O_2;H_2}$ difference equals 1.35 V for La_3Ni and 1.36 V for $LaNi_5$ electrode. This means that exchange current density of O_2/OH^- system is clearly smaller (*ca* 1.5–1.8 orders of magnitude) than that for H_2O/H_2 system for both electrode materials.

4 Conclusions

Galvanostatic $-i/+i$ measurements of electrode potential versus time allow to evaluate precisely the effectiveness of cathodic hydrogen absorption by the tested alloy in strong alkaline solution. The galvanostatic $-i/+i$ method is also very useful to determine exchange current density of H_2O/H_2 system on the surface of the alloy which is able to absorb cathodically evolved hydrogen. Precise determination of both effectiveness of hydrogen absorption and exchange current density of H_2O/H_2 system is possible not only for electrodes absorbing large quantities of cathodic hydrogen (e.g. $LaNi_5$) but also for material showing poor hydrogen absorption abilities as well (e.g. La_3Ni). The galvanostatic method brings about correct results unless the anodic current of the tested material in passive region i_{pas} is greater than the absolute value of external $-i/+i$ current.

References

1. Iwakura C, Matsuoka M (1991) Prog Batter Battery Mater 10:81
2. Bechman CA, Goudy A, Takeshita T, Wallace WE, Craig RS (1976) Inorganic Chem 15:2184
3. Levin EE, Safonova TYa, Petrii OA (2006) J New Mater Electrochem Syst 9:155
4. Huang YC, Tada M, Watanabe T, Fujita K (1979) Proceedings of the 2nd World hydrogen energy conference. Pergamon Press, Oxford, Zurich
5. Luo S, Luo W, Clewley JD, Flanagan T, Wade LA (1995) J Alloys Comp 231:467
6. Rożdżyńska-Kielbik B, Iwasieczko W, Drulis H, Pavlyuk VV, Bala H (2000) J Alloys Comp 298:237
7. Giza K, Bala H, Pavlyuk VV, Iwasieczko W, Drulis H (2008) Phys-Chem Mech Mater 7:139 (special issue)
8. Giza K, Iwasieczko W, Bala H, Pavlyuk VV, Drulis H (2009) Int J Hydrogen Energy 34:915
9. Witham C, Hightower A, Fultz B, Ratnakumar BV, Bowman RC Jr (1997) J Electrochem Soc 144:3758
10. Mal HH, Buschow KHJ, Miedema AR (1974) J Less-Common Met 35:65
11. Li Y, Han S, Li J, Zhu X, Hu L (2008) J Alloys Comp 458:357
12. Oh JW, Kim CY, Nahm KS, Sim KS (1998) J Alloys Comp 278:270
13. Meisner GP, Panchanathan V (1993) J Appl Phys 73:6482
14. Mu D, Hatano Y, Abe T, Watanabe K (2002) J Alloys Comp 334:232
15. Rangel CM, Fernandes VR, Slavkov Y, Bozukov L (2008) J Power Sources 181:382
16. Giza K, Bala H, Owczarek E, Rożdżyńska-Kiełbik B, Pavlyuk VV (2007) Ochr przed Korozja 50:162 (special issue)
17. Zakroczymski T, Owczarek E (2002) Acta Mater 50:2701
18. Addach H, Bercot P, Rezrazi M, Takadoum J (2009) Corros Sci 51:263

19. Hu WK, Shen PW, Shang YS, Wang GS, Song DY, Zhou ZX (1995) Int J Hydrogen Energy 20:245
20. Rożdżyńska-Kiełbik B, Bala H, Pavlyuk VV (2004) Ochr przed Korozja 47:167 (special issue)
21. Rożdżyńska-Kiełbik B, Bala H, Giza K (2007) Ochr przed Korozja 50:175 (special issue)
22. Giza K, Bala H, Rożdżyńska-Kiełbik B (2008) Inż Materiałowa 29:1025
23. Williams AJ, McGuinness PJ, Harris IR (1990) IEEE Trans Magn 26:1946
24. Christodoulou CN, Takeshita TJ (1993) Alloys Comp 191:279
25. Chang KE, Warren GW (1994) J Appl Phys 76:6262
26. Bittner HF, Badcock CC (1983) J Electrochem Soc 130:193c
27. Chang KE, Warren GW (1995) IEEE Trans Magn 31:3671
28. Giza K, Bala H, Pavlyuk VV (2009) Mater Corros 60:29
29. Bond GC (1974) Heterogeneous catalysis: principles and applications. Clanderon Press, Oxford
30. Notten PHL, Hokkeling P (1991) J Electrochem Soc 138:1877
31. Senoh H, Ueda M, Inoue H, Furukawa N, Iwakura C (1998) J Alloys Comp 266:111
32. Meli F, Zuttel A, Schlapbach L (1995) J Alloys Comp 192:155
33. Kukula I, Bala H, Marciniak B, Pavlyuk VV (2009) Ochr przed Korozja 52(4): 202
34. Kiss L (1988) Kinetics of electrochemical metal dissolution. Akad Kiado, Budapest
35. Stern M, Geary AL (1957) J Electrochem Soc 104:56
36. Rożdżyńska-Kiełbik B, Bala H, Pavlyuk VV (2005) Ochr przed Korozja 48:35 (special issue)
37. Habashi M (1990) In: Desjardins D, Oltra R (eds) Corrosion sous contrainte. Phenomenologie et mecanismes. Éditions de Physique, Bombannes, France
38. San Marchi C, Somerday BP, Robinson SL (2007) Int J Hydrogen Energy 32:100
39. Giza K, Bala H, Pavlyuk VV (1999) Ochr przed Korozja 42:477 (special issue)
40. Giza K, Bala H, Pavlyuk VV, Drulis H, Iwasieczko W (2002) Inż Materiałowa 23:623